[4] K. T. Lay and A. K. Katsaggelos, "Image identification and restoration based on the expectation-maximization algorithm," *Opt. Eng.*, vol. 29, pp. 436–445, May 1990.
[5] R. L. Lagendijk, J. Biemond, and D. E. Boekee, "Identification and restoration of noisy blurred images using the expectation-maximization algorithm," *IEEE Trans. Acoust., Speech, Signal Processing*, vol. 38, pp. 1180–1191, July 1990.
[6] ——, "Hierarchial blur identification," in *Proc. IEEE Int. Conf. Acoust., Speech, Signal Processing*, 1990, pp. 1889–1892.
[7] R. L. Lagendijk, A. M. Tekalp, and J. Biemond, "Maximum likelihood image and blur identification: A unifying approach," *Opt. Eng.*, vol. 29, pp. 422–435, May 1990.
[8] J. Kim and J. W. Woods, "Image identification and restoration in the sub-band domain," *IEEE Trans. Image Processing*, vol. 3, pp. 312–314, May 1994.
[9] A. K. Katsaggelos and R. W. Schafer, "Iterative deconvolution using several different distorted versions of an unknown signal," in *Proc. IEEE Int. Conf. Acoustics, Speech, Signal Processing*, Boston, MA: 1983, pp. 659–662.
[10] D. C. Ghiglia, "Space-invariant deblurring given N independently blurred images of a common object," *J. Opt. Soc. Amer. A*, vol. 1, pp. 398–402, Apr. 1984.
[11] R. K. Ward, "Restoration of differently blurred versions of an image with measurement errors in the PSF's," *IEEE Trans. Image Processing*, vol. 2, pp. 369–381, July 1993.
[12] A. N. Rajagopalan and S. Chaudhuri, "Maximum likelihood estimation of blur from multiple observations," in *Proc. IEEE Int. Conf. Acoustics, Speech, Signal Processing*, Munich, Germany, Apr. 1997, pp. 2577–2580.
[13] M. Subbarao, "Efficient depth recovery through inverse optics," in *Machine Vision for Inspection and Measurement*, H. Freeman, Ed. New York: Academic, 1989.
[14] F. A. Graybill, *An Introduction to Linear Statistical Models.* New York: McGraw-Hill, 1961, vol. 1.
[15] A. N. Rajagopalan and S. Chaudhuri, "Space-variant approaches to the recovery of depth from defocused images," *Computer Vision and Image Understanding*, to be published.
[16] ——, "Optimal selection of camera parameters for recovery of depth from defocused images," in *Proc. IEEE Int. Conf. Computer Vision and Pattern Recognition*, U.S. Virgin Islands, June 1997.

Region Growing: A New Approach

S. A. Hojjatoleslami and J. Kittler

***Abstract*— A new region growing method for finding the boundaries of blobs is presented. A unique feature of the method is that at each step, at most one pixel exhibits the required properties to join the region. The method uses two novel discontinuity measures, *average contrast* and *peripheral contrast,* to control the growing process.**

I. Introduction

The segmentation of regions is an important first step for a variety of image analysis and visualization tasks. There is a wide range of image segmentation techniques in the literature, some considered general purpose and some designed for a specific class of images. Conventional segmentation techniques for monochromatic images can be categorized into two distinct approaches [3]. One is region based, which relies on the homogeneity of spatially localized features, whereas the other is based on boundary finding, using discontinuity measures. The two methods exploit two different definitions of a region which should ideally yield identical results. Homogeneity is the characteristic of a region and nonhomogeneity or discontinuity is the characteristic of the boundary of a region. Based on one or both of these properties, diverse approaches to image segmentation exhibiting different characteristics have been suggested [1], [2], [4], [8]–[10], [12], [13].

We present here a new idea for region growing by pixel aggregation, which uses new similarity and discontinuity measures. A unique feature of the proposed approach is that in each step at most one candidate pixel exhibits the required properties to join the region. This makes the direction of the growing process more predictable. The procedure offers a framework in which any suitable measurement can be applied to define a required characteristic of the segmented region. We use two discontinuity measurements called *average contrast* and *peripheral contrast* to control the growing process. Local maxima of these two measurements identify two nested regions, called the *average contrast* and the *peripheral contrast* regions. The method first finds the average contrast boundary of a region, then a reverse test is applied to produce the peripheral contrast boundary.

Like existing procedures, the method proposed in this paper is not universal, but it does appear to have a fairly wide application potential, especially in medical image analysis, where the areas corresponding to a tissue of interest appear as bright/dark objects relative to the surrounding tissues.

The concept of the method is presented in the next two sections. The similarity measure used by the method is presented in Section II. Section III introduces the two different discontinuity measures, *peripheral contrast* and *average contrast,* and illustrates their behavior on a Gaussian shape image. The capability of our method is then demonstrated on a set of real images in Section IV, followed by a summary and conclusion in Section V.

II. Growing Process

The concept of our method, like that of other region growing methods by pixel aggregation, is to start with a point that meets a detection criterion and to grow the point in all directions to extend the region.

Let us assume that the process starts from an arbitrary pixel. The pixel is labeled as a region that then grows based on a similarity measure. In our approach, a boundary pixel is joined to the current region provided it has the highest grey level among the neighbors of the region. This induces a directional growing such that the pixels of high grey level will be absorbed first. When all the high grey level pixels in the region are absorbed, the process continues by absorbing the boundary pixels with monotonically lower and lower grey levels. When several pixels with the same grey level jointly become the candidates to join the region, the first-come first-served strategy is used to select one of them. This makes the region more compact, particularly in situations where the grey levels of the background or the region pixels are very homogeneous.

In order to monitor the pixels joining the region, a grey-level mapping is generated. The mapping is very similar to the mapping of data points from a high-dimensional feature space onto a sequence which is used in the mode separating (MODESP) procedure for cluster analysis proposed by Kittler [7]. The mapping for a small

Manuscript received November 5, 1995; revised October 27, 1997. The associate editor coordinating the review of this manuscript and approving it for publication was Prof. Patrick A. Kelly.

The authors are with the Centre for Vision, Speech and Signal Processing, University of Surrey, Guildford, Surrey GU2 5XH, U.K. (e-mail: a.hojjatoleslami@ee.surrey.ac.uk).

Publisher Item Identifier S 1057-7149(98)04449-2.

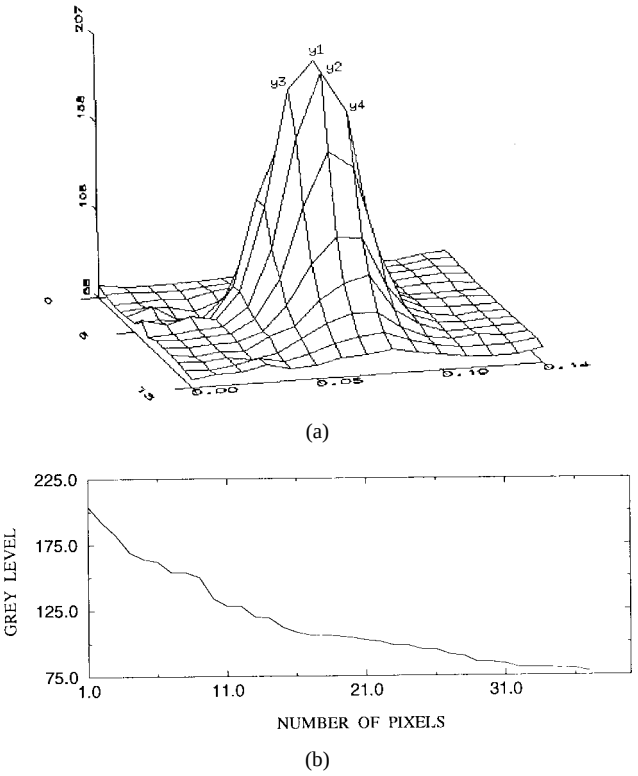

Fig. 1. (a) Topographical surface of a microcalcification in a homogeneous background. (b) Mapping of grey levels of the region during the growing process.

subimage with a single bright blob is shown in Fig. 1(a). To present the concept of the growing process on this data, let us assume that its starting point y_1 is the pixel with the maximum grey level of the subimage. The pixel defines a nucleus of the blob region. The sequence of pixels joining the region is y_2, y_3, y_4, and so on. The graph of the grey levels associated with the sequence of candidate pixels for the region is shown in Fig. 1(b). The mapping shows that the grey levels decrease from the high values in the region to low values in the background.

A similar mapping function can be defined on the sequence of pixels joining the growing region to characterize the variation of the measurements in the spatial domain. A suitable coarse criterion is used to stop the growing process and to apply a reverse check on the relevant measurements to detect the region boundary. We use the maximum possible size N of a region to stop the process. However, other criteria, such as the minimum size of the neighboring region, or the maximum difference between the current candidate and the maximum grey level inside the region can also be applied to stop the growing process [5]. The size of a region is simply measured by counting the number of pixels in the mapping. Accordingly, the index number i of the current pixel must satisfy

$$i < N \tag{1}$$

where N is the maximum expected size (number of pixels) of the grown region.

III. Discontinuity Measures

For segmentation purposes we define a region of interest as a grey-level blob, exhibiting a high contrast relative to its local background. The best boundary for the region is a set of connected pixels exhibiting predefined contrast properties. We use two different properties for each region, called *average contrast* and *peripheral contrast*, to define its nested boundaries.

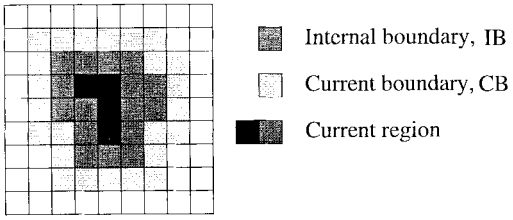

Fig. 2. Schematic graph shows the CB, including candidate pixels to be joined to the region, and IB, including the outermost pixels of the region, during the growing process. The region contains 20 pixels.

In order to define the two region measurements we shall introduce the following terminology. *Current boundary* (CB) is the set of pixels adjacent to the current region. *Internal boundary* (IB) is defined as the boundary produced by the set of connected outermost pixels of the current region. The two concepts are illustrated in Fig. 2. The current region and the two boundaries, CB and IB, are dynamically changing during the growing process.

Using this terminology, the *average contrast* measure $c(i)$ for a region containing i pixels is defined as the difference between the average grey level of the region and the average of its CB pixels, i.e,

$$c(i) = \frac{1}{i}\sum_{t=1}^{i} y_t - \frac{1}{k-i}\sum_{t=i+1}^{k} y_t \tag{2}$$

where $y_1, y_2, \cdots, y_i$ is the sequence of pixels forming the current region and $y_{i+1}, y_{i+2}, \cdots, y_k$ is the set of its CB pixels.

The region growing will produce increasing average contrast measure values as long as the growing region continues subsuming high intensity pixels of the bright blob. Once it starts growing into the background, the rate of grey-level decrease for the boundary will be less than that for its region, and consequently the average contrast will commence decreasing. Hence, the maximum of this measurement during the growing process corresponds to the point when the process starts to grow into the background. The result of the segmentation based on the maximum average contrast is the *average contrast boundary* (ACB) of the region.

We define the *peripheral contrast* of a region as the difference between the grey level average of the current IB and the average of the CB. The peripheral contrast reflects an average magnitude of the gradient of the pixels in the CB of the evolving region. It is less sensitive to noise than the measurement of a pixel gradient magnitude as it uses the difference between two neighboring boundaries rather than that of two neighboring pixels. Note that for a relatively homogeneous region, the global maximum of the peripheral contrast will be uniquely defined. However for noisy or textured regions the peripheral contrast will exhibit many local peaks. Each such peak can be used to segment out a distinct region which will meaningfully correspond to the information conveyed by the internal part of the region. In order to counter act the multiplicity of solutions caused by the effect of noise or texture on the peripheral contrast, we use the last local maximum of the peripheral contrast occurring before the maximum of the average contrast measure to determine the *peripheral contrast boundary* (PCB). We advocate the use of peripheral contrast as the final result of segmentation.

Commonly, the ACB and the actual boundary (PCB) are not very far away from each other, especially when strong edges exist. The difference may be large for fuzzy edge regions. We shall illustrate the difference between the two boundaries on an isotropic Gaussian blob image that has a very extensive ACB as compared to its PCB.

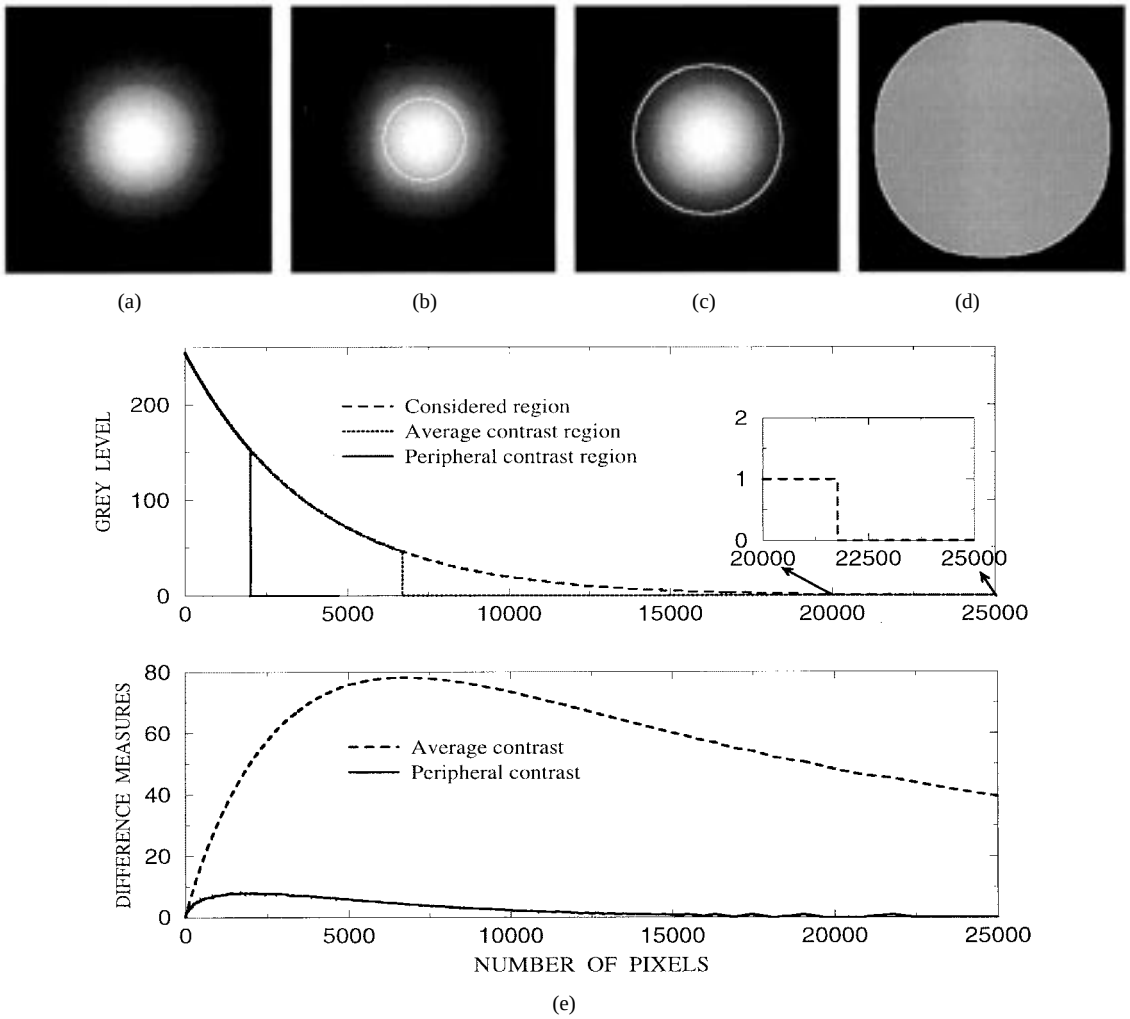

Fig. 3. Segmentation results for a Gaussian shape image with $\sigma = 25$. The region size criterion used is $N = 25\,000$. (a) Original image. (b) Segmentation result, PCB, based on the peripheral contrast measure. (c) ACB segmented by the maximum average contrast point. (d) The boundary produced by the maximum size threshold (25000 pixels). (e) Grey level, peripheral contrast and average contrast mappings obtained during the growing process.

Equation (3) defines such a two-dimensional (2-D) Gaussian shape

$$g(x, y) = M \exp^{-(1/2)[((x-u_x)^2/\sigma^2)+(y-u_y)^2/\sigma^2)]} \tag{3}$$

where u_x, u_y specify the x, y location of the centre of the Gaussian blob and σ specifies the spread of the grey-level function. Constant M is used to normalize the output to the maximum grey-level range.

It can be easily shown that the highest gradient magnitude of the Gaussian shape which is approximated by the peripheral contrast is located one standard deviation from the mean. Thus the maximum peripheral contrast measure for the Gaussian shape specifies a circle with radius σ, centered at coordinates $[u_x, u_y]$.

A Gaussian shape image with a standard deviation of 25 pixels, $\sigma = 25$, shown in Fig. 3(a), is used to demonstrate the relationship of the two boundaries. Let the growing process start at the highest grey level in the region, 255. The grey-level mapping in Fig. 3(e) shows that the grey levels of the sequence of pixels joining the region monotonically decrease to zero, which corresponds to the background. As a result of the directional growing process, the shape of the region for the Gaussian shape is circular even when the process continues to absorb the zero grey levels in the background. This is apparent by considering Fig. 3(d) and noting that the grey level of all the candidate pixels beyond pixel number 21 772 is zero. As one might expect, average contrast commences from a low value and smoothly increases to a maximum at point 6685 and then decreases. The maximum average contrast point in the Gaussian image defines a circular region with the radius of approximately 1.85σ, shown in Fig. 3(c).

The mapping of *peripheral contrast* starts from low value increasing to a maximum at pixel number 2000 and then decreasing again to zero. The maximum peripheral contrast point corresponds to a circular region with the radius of approximately 1.01 σ in the Gaussian image, shown in Fig. 3(b). This result agrees well with the maximum gradient region of a continuous Gaussian shape. The slight difference is caused by the effect of quantization and the fact that our method uses the difference between the mean of two completely closed contour boundaries to calculate the peripheral contrast, so the effect of diagonal pixels the distance of which is $\sqrt{2}$ is the same as that of pixels located in the adjacent position with distance one.

IV. Experiments on Real Images

This section shows the performance of our method on medical images where each region can be categorized as a bright blob separated from its neighbors by a boundary of lower grey level. We show that our method is not sensitive to threshold N of rule (1) and discuss the grey-level average contrast and peripheral contrast mappings when N is too high in comparison to the size of the region of interest.

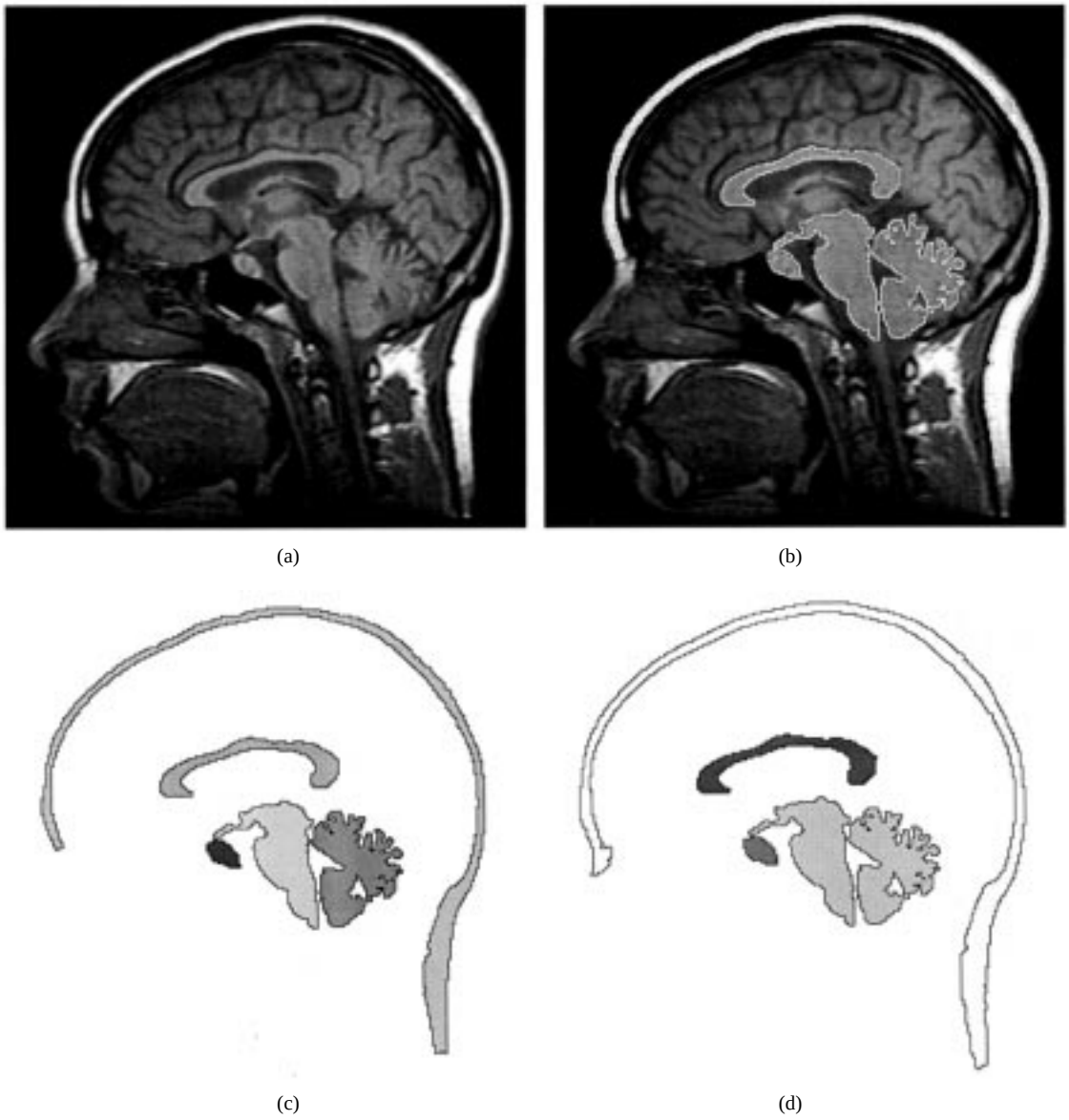

Fig. 4. (a) Original MR image of head. (b) Segmentation result of five regions superimposed on the original image. (c), (d) peripheral contrast and average contrast regions and boundaries segmented out from image (a).

Consider the magnetic resonance (MR) image of a head shown in Fig. 4(a). A very high threshold, $N = 20000$, in comparison to the size of the region of interest is used to provide an opportunity to consider the behavior of the discontinuity measurements in relation to the neighboring regions. The grey level and contrast mappings obtained during the growing process are shown in Fig. 5. The highest average contrast at pixel index 4604 determines the location of the ACB and the last peripheral contrast measure maximum before the maximum average contrast point specifies the final boundary for the region. The regions segmented out using the method are shown in Fig. 4(b)–(d).

The grey-level mapping shows local valleys that are induced by the grey levels at the boundary of two neighboring regions. Each visible valley in the grey-level mapping is the result of the switch between the absorption of decreasing grey levels of the pixels in the boundary of the region being grown and the absorption of pixels of increasing grey levels leading to the nearest local peak of the neighboring region. The gradient on the right side of the valley is related to the rate of grey-level increase along the pathway forged by the growing process toward a local hill. Thus, the difference between a valley minimum and the following peak in the grey-level mapping shows the difference between the maximum grey level of the hill and the maximum grey level at which the two neighboring regions meet. If the difference is quite high and the number of pixels in the new region is large enough, it is a strong clue for the existence of a new significant region. Otherwise, the new hill is a local peak or noise in the region being grown. Such variations also produce relevant peaks and valleys in the two contrast mappings (see Fig. 5).

Five distinct parts of the MR image segmented based on the average contrast and peripheral contrast peaks are shown in Fig. 4. For each segmented region in the image, a starting point is selected. We tested the algorithm using every starting point in the five regions, but the segmentation results were the same (there was zero difference between the results produced by any starting point inside a region). The independence of the segmentation results from the choice of a starting point is an important characteristic of the approach.

In another experiment, we examined the performance of the method on the MR image when Gaussian noise was added to the original

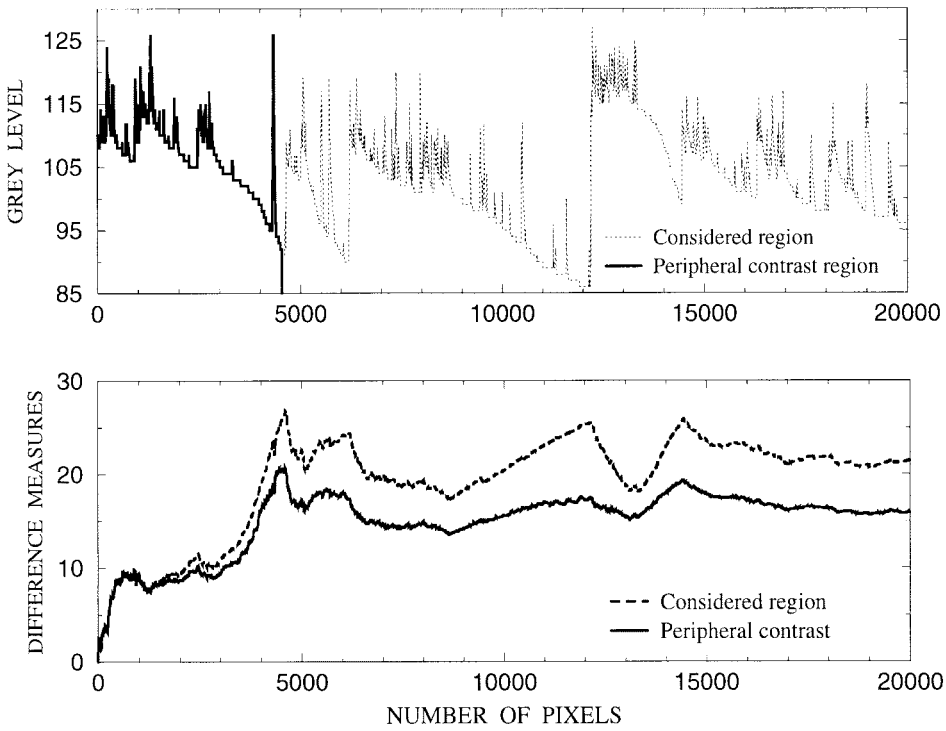

Fig. 5. The mappings for brain-stem during the growing process starting at pixel (304, 165), $N = 20\,000$.

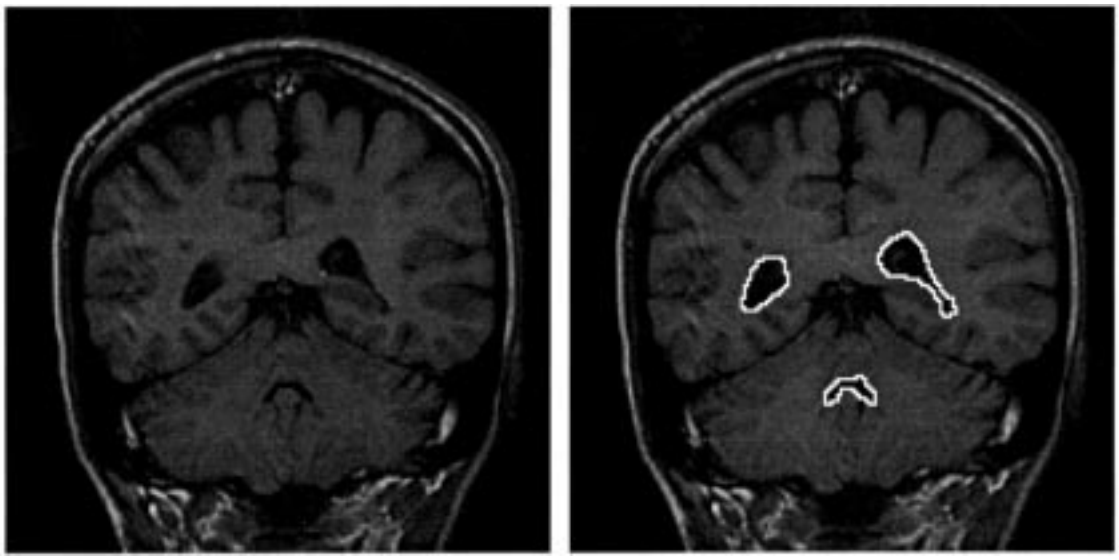

Fig. 6. Segmentation of cavities in the brain.

image. The segmentation results obtained on the noisy image were compared with the results produced by applying the method to the original image. The segmentation error rate is defined by the percentage of pixels incorrectly labeled by the region growing method and for a given noise level, it is averaged over different noise sequences. The error for various levels of standard deviation, σ, of the Gaussian noise for the five regions in the MR image is plotted in Fig. 7. The error rate for scalp is very low, less than 10%, even when $\sigma = 20$. This is because of the relatively sharp edge between the scalp and other tissues. The error rate as a function of noise is much higher for cerebellum and corpus callosum and pituitary gland. High sensitivity of the method to the noise for those regions is caused by the relatively low contrast between the tissues and their background (fuzzy edges) and by being located in a close vicinity to neighboring regions. The latter is particularly important, as occurrence of noisy grey-level pixels of high intensity at the boundary between two neighboring regions may cause the two regions to join. In such situations, application specific measurements like shape measures can be applied to prevent the growing process from absorbing the neighboring regions.

The above discussion is also applicable to segment out a dark region from a brighter background if the whole process is reversed. In such a case, the minimum peripheral contrast measure defines the final boundary for the dark region. This is demonstrated by applying the method to segment out the cavities in another MR image, shown in Fig. 6(a). The segmentation results of our method using three

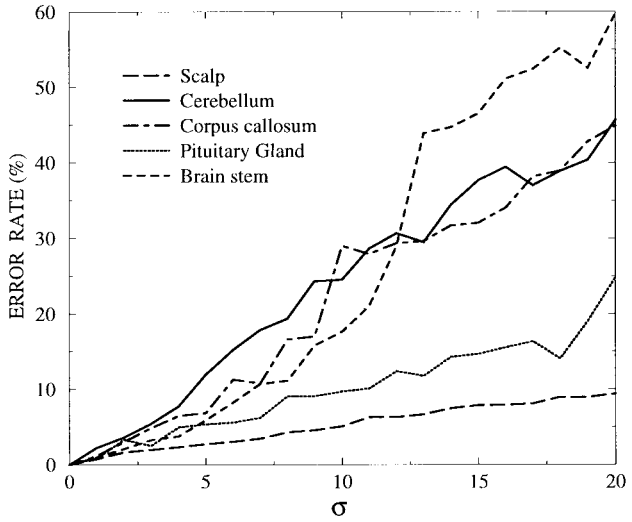

Fig. 7. Segmentation error of the regions in the MR image for different level of Gaussian noise.

arbitrary starting points, one in each cavity, are shown in Fig. 6(b). The results are again in full agreement with the results of human visual segmentation.

V. Summary and Conclusions

A new method of region growing by pixel aggregation, using novel similarity and discontinuity measures, has been presented. The unique feature of the proposed approach is that in each step at most one candidate pixel will exhibit the required properties to join the region. This makes the direction of the growing process more predictable. Two new discontinuity measures, average contrast and peripheral contrast, which use grey-level difference information to produce the final segmentation result, are proposed, and their properties analyzed. The use of the two discontinuity measures guarantees the robustness of our region growing approach to intensity changes. This contrasts with the sensitivity to grey-level shifts commonly exhibited by conventional region growing techniques [4], [6], [13].

Since the growing process is directional, i.e., pixels join the grown region according to a ranking list, the method does not necessarily include all the pixels with the same grey level to the region. This contrasts with thresholding methods where all the pixels exceeding a certain threshold are included in the segmented region [11]. From an extensive experimental testing, our method appears to be more reliable and consistent than other region growing and thresholding methods when the aim is the segmentation of bright objects from a dark background or vice versa [4], [6], [11].

References

[1] A. J. Abrantes and J. S. Marques, "A class of constrained clustering algorithms for object boundary extraction," *IEEE Trans. Image Processing*, vol. 5, pp. 1507–1521, 1996.
[2] R. Adams and L. Bischof, "Seeded region growing," *IEEE Trans. Pattern Anal. Machine Intell.*, vol. 16, pp. 641–647, 1994.
[3] D. H. Ballard and C. Brown, *Computer Vision.* Berlin, Germany: Springer Verlag, 1982.
[4] R. M. Haralick and L. G. Shapiro, "Survey: Image segmentation techniques," *CVGIP*, vol. 29, pp. 100–132, 1985.
[5] S. A. Hojjatoleslami and J. Kittler, "Automatic detection of calcification in mammograms," *IEE 5th Int. Conf. Image Processing and Its Applications*, 1995, pp. 139–143.
[6] H. Jiang, J. Toriwaki, and H. Suzuki, "Comparative performance evaluation of segmentation methods based on region growing and division," *Syst. Comput. Jpn.*, vol. 24, no. 13, pp. 28–42, 1993.
[7] J. Kittler, "A locally sensitive method for cluster analysis," *Pattern Recognit.*, vol. 8, pp. 23–33, 1976.
[8] L. Najiman and M. Schmitt, "Geodesic saliency of watershed contours and hierarchical segmentation," *IEEE Trans. Pattern Anal. Machine Intell.*, vol. 18, pp. 1163–1173, 1996.
[9] N. R. Pal and S. K. Pal, "A review on image segmentation techniques," *Pattern Recognit.*, vol. 26, pp. 1277–1294, 1993.
[10] T. Pavlidis and Y.-T. Liow, "Integrating region growing and edge detection," *IEEE Trans. Pattern Anal. Machine Intell.*, vol. 12, pp. 225–233, 1990.
[11] P. K. Sahoo, S. Soltani, and A. K. C. Wong, "A survey of thresholding techniques," *CVGIP*, vol. 41, pp. 233–260, 1988.
[12] M. Tabb and N. Ahuja N, "Multiscale image segmentation by integrated edge and region detection," *IEEE Trans. Image Processing*, vol. 6, pp. 642–655, 1997.
[13] X. Yu and J. YlaJaaski, "A new algorithm for image segmentation based on region growing and edge detection," *Proc. Int. Symp. Circuits and Systems*, 1991, vol. 1, pp. 516–519.

Fuzzy Homogeneity Approach to Multilevel Thresholding

H. D. Cheng, C. H. Chen, H. H. Chiu, and Huijuan Xu

***Abstract*—The spatial ambiguity among pixels has inherent vagueness rather than randomness, therefore, the conventional methods might not work well. We propose fuzzy homogeneity vectors to handle the grayness and spatial uncertainties among pixels, and to perform multilevel thresholding. The experimental results prove that the proposed approach works better than the histogram-based algorithms.**

***Index Terms*—Fuzzy entropy, fuzzy homogeneity, image thresholding.**

I. Introduction

Image thresholding has wide applications in many areas, and there are many methods for thresholding [1]–[4]. Spatial distribution among pixels in an image is one aspect of texture used for image thresholding and classification. In terms of image processing, due to the deficiency of specificity and the fuzziness of boundaries, the advantages provided by fuzzy set theory are characterized by various definitions of membership functions associated with the pixels rather than the definitions provided by the crisp set theory [5], [6]. In the previous work [5], [7], the fuzzy set theory has been employed for image thresholding; however, the fuzzy region width was determined heuristically, and the measures of texture were computed using only histograms that suffer from the limitation that they carry no spatial information of pixels with respect to each other. To overcome this shortcoming, we propose the fuzzy homogeneity vector to determine the fuzzy region width and calculate the fuzzy entropies. It not only takes into account of the advantage of the fuzzy framework, but also

Manuscript received March 13, 1996; revised October 20, 1997. The associate editor coordinating the review of this manuscript and approving it for publication was Prof. Jeffrey J. Rodriguez.

The authors are with the Department of Computer Science, Utah State University, Logan, UT 84322-4205 USA (e-mail: cheng@hengda.cs.usu.edu).

Publisher Item Identifier S 1057-7149(98)04373-5.